View metadata, citation and similar papers at core.ac.uk
brought to you by CORE
provided by Institute of Transport Research:Publications

Functional Integrated Sandwich Structures for Vehicle Concepts of the Next Generation

S.Brückmann[1], G.Kopp[2], M.Kriescher[3], H.E.Friedrich[4]
J.Laskowski[5], B.Milow[5], L.Ratke[5], A. Orth[6]
[1,2,3,4]Institute of Vehicle Concepts, 70569 Stuttgart, Germany
[5]Institute of Materials Research, DLR, 51147 Cologne, Germany
[6]Institute for Space Operations and Astronaut Training, DLR, 51147 Cologne, Germany
simon.brueckmann@dlr.de, gundolf.kopp@dlr.de, michael.kriescher@dlr.de, horst.friedrich@dlr.de
jessica.laskowski@dlr.de, barbara.milow@dlr.de, lorenz.ratke@dlr.de, andreas.orth@dlr.de

Keywords: Functional Integration, Lightweight Design, Sandwich Design, Crash Behavior, Polyurethane Foam, Aerogels, Aerofims, Vehicle Concept

State of the Art

In an age of global climate change, reducing the emission of greenhouse gases and pollutants is essential in order to slow down continuing climate warming. Moreover, the shortage of resource is also an important aspect which has to be considered in the development of new vehicles or vehicle components. Steady population growth and the increasing need for mobility associated with it will in future continue to exacerbate the situation with regard to the emission of greenhouse gases and pollutants. These factors, plus the statutory requirements, allow the conclusion that reductions in the consumption and emission values of passenger cars are essential. The main way of achieving this is by improving the efficiency of vehicles. As well as improving aerodynamics and the power train, increasing efficiency is possible through lightweight design, since a large proportion of fuel consumption is generated by the vehicle mass. The mass-dependent fuel consumption of passenger cars is detailed in Fig. 1.

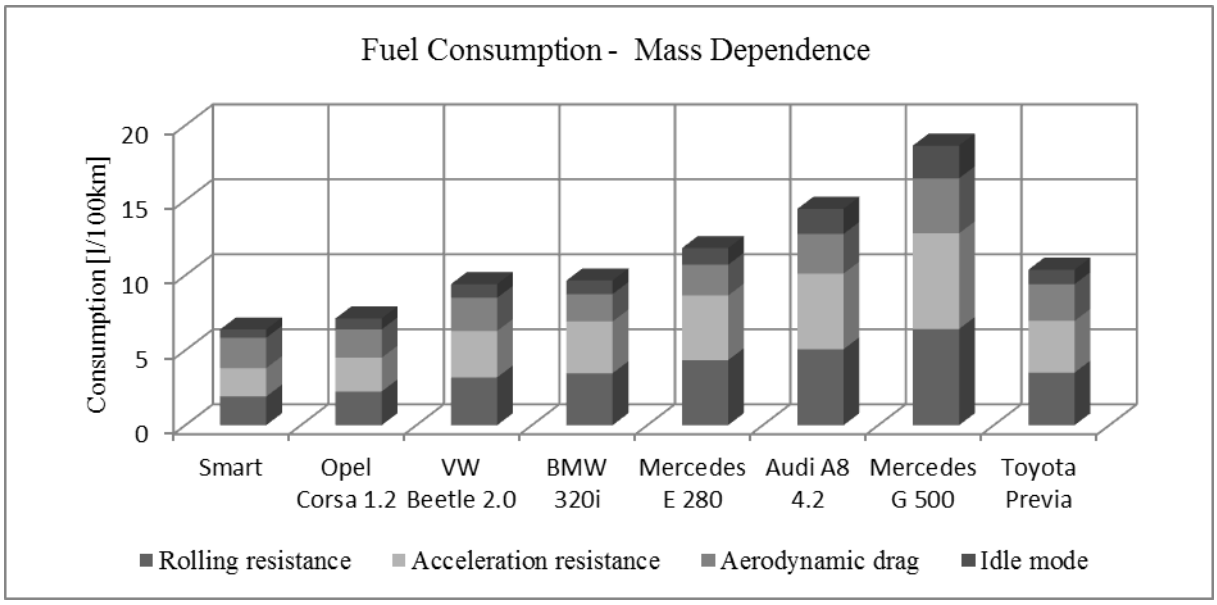

Fig. 1: Fuel consumption of different vehicles; mass dependence [1]

The share of consumption due to aerodynamic drag and idling consumption is around 30 to 40% of total consumption, whereas the mass-dependent consumption of a vehicle due to rolling and acceleration resistance is up to 70%. These values are irrespective of the total vehicle mass (cf. Fig. 1). It is therefore evident that by saving on mass, a large proportion of consumption can be influenced

and that the type and the mass of vehicle being investigated are irrelevant. In vehicles with an alternative drive, e.g. electrically driven vehicles, a reduction in the mass of the body in white structure is of considerable importance, because electrical energy storage systems are heavy. There are various lightweight design strategies for reducing vehicle mass, e.g. sandwich construction. These include conditional, conceptual, material and form lightweight construction. These options of reducing vehicle mass, in combination with sandwich construction, open up further potential to reduce mass. This includes, for example, the integration of additional functions such as the insulation of the vehicle interior or crash improvements. One example of a sandwich structure can be constructed from cover layers (e.g. aluminum), adhesive and core material (e.g. polyurethane foam, aerogels). The cover layers of a sandwich composite mainly absorb tensile and compressive forces. Forces at panel level are distributed two-dimensionally onto the core, so that where the design is optimal no local weakening is created. Furthermore, the cover layer material should possess a high Young's modulus, good impact resistance, high surface quality and high wear resistance [2]. The core material serves to absorb thrust and to guarantee the spacing of the cover layers. Moreover, in most cases it has a low density, possesses high shearing strength, a high degree of stiffness in the direction of the cover layer and often a good thermal insulation effect [2]. Because of the thickness of a sandwich structure, the geometrical moment of inertia of the structure is high compared with an orthodox sheet metal structure with approximately the same mass. Consequently, when the structure thickness is quadrupled, stiffness and bending strength increase by a factor of 37 and 9.2 respectively, whereas the mass only increases by around 6% (cf. Fig. 2).

	Stiffness	Bending strenght	Mass
Only layers	1,0	1,0	1,0
Core thickness t	7,0	3,5	1,03
Core thickness 3t	37,0	9,2	1,06

Fig. 2: Comparison of stiffness, bending strength and mass of a sheet and two sandwich configurations [3]

Investigation of generic polyurethane foam samples

The aim of the investigations was the applicability of sandwich materials in vehicle areas affected by cases of crash load. The analytical design of sandwich elements is only possible if foam behavior is known. For this reason, different models were investigated in order to calculate the Young's modulus and the yield strength of the foams and then compared with the manufacturer data. The comparison produces considerable differences. This connection becomes clear in Figs. 3 and 4. Especially in high density areas (200 kg/m³), a difference of over 70% in the Young's modulus and over 100% in the yield strength can be seen.

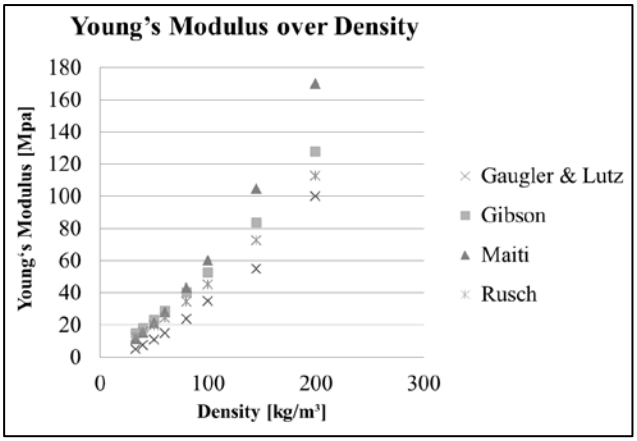

Fig. 3: Young's modulus over density: comparison of manufacturer data (Gaugler & Lutz) with analytically calculated values

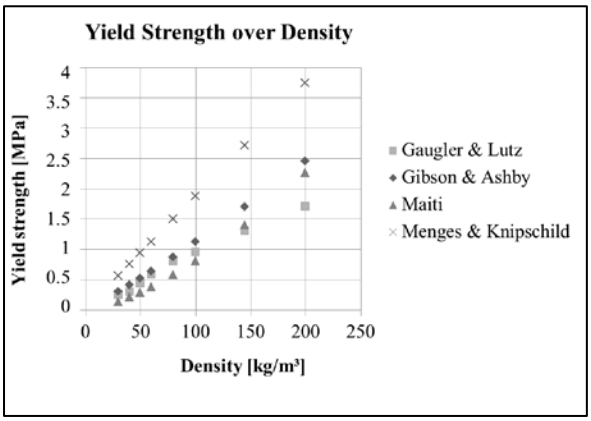

Fig. 4: Yield strength over density: Comparison of manufacturer data with analytically calculated values

In the case of a foam density of 100 kg/m³, the manufacturer data for Young's modulus agrees with the calculated values according to Menges & Knipschild. In the case of a foam density above 100 kg/m³, all calculated values are above the manufacturer data quoted here. Below this foam density, the calculated values according to Menges & Knipschild are lower than those of the manufacturer. A similar connection can be seen for yield strength. Here, in the lower density range, the calculation values according to Maiti are below, and in the upper range above the manufacturer data. A comparison of the various calculation models with the manufacturer parameters allows the conclusion that generic tests on different polyurethane foams must be carried out. The foams are stressed for compression, tension and shear strain. The parameters of Young's modulus, shear modulus, compression strength, tensile strength and shear resistance were determined. In addition, force-displacement diagrams of the test piece series were prepared, in order to be able to add them to FE models.

All stress-strain diagrams produced, which were determined during the static compression tests, possess the shape shown by way of example in Fig. 5. At the end of the linear-elastic phase a local stress peak occurs in the gradient, followed by a stress drop to the plateau phase. This stress drop indicates that the first cell walls of the foam are collapsed. In the plateau phase, the approximate plasticization stress of the foam is read off. In this phase further foam cells collapse continuously. After this follows the compression phase, in which the foam is compressed to the final value of 85% compression (cf. DIN EN ISO 844 [4]).

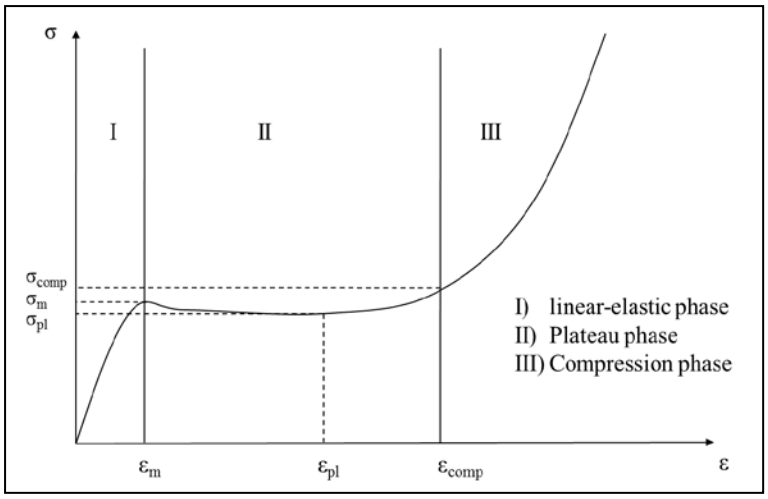

Fig. 5: Stress-strain diagram of foam, example

The results of the compression and tensile tests are shown in Fig. 6. Shown in the left-hand diagram is the tensile strength, in the middle diagram the secant modulus and in the right-hand diagram the elastic compression limit. The tensile test was carried out in accordance with DIN 53292 [5]. Whereas the curve progressions of the secant modulus and of the elastic compression limit exhibit an exponential gradient, the tensile strength of the foams increases in linear fashion with the density. The physical test data generated is required for extrapolating the tests to generic sandwich elements. On the basis of the material parameters determined, the cover layer and core thicknesses can be calculated and a selection made as to which foam density is appropriate in the sandwich composite.

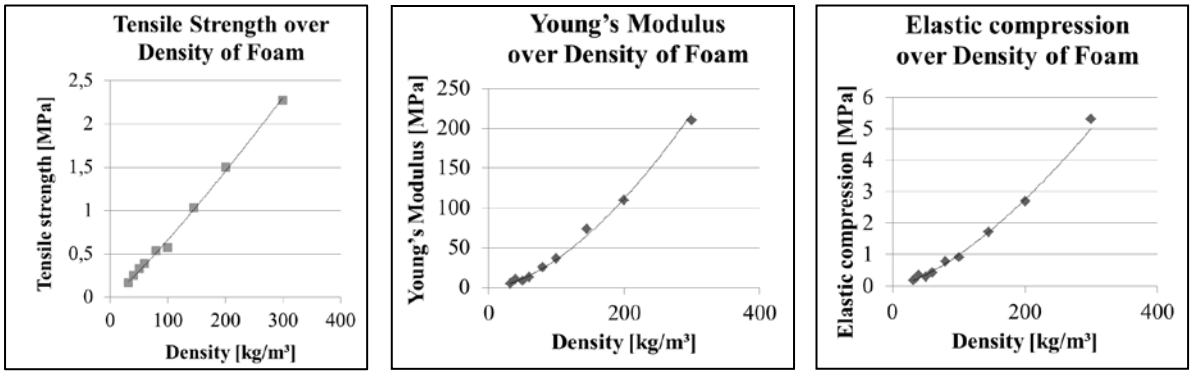

Fig. 6: Results: Top right: Young's modulus, left middle: elastic compression, bottom right: tensile strength; overall density of foam

Generic sandwich elements

Using generic sandwich elements, the influence of cover layer thickness, foam density and core thickness on the failure behavior of the test pieces was investigated. In Fig. 7, three different failure modes are shown. On the left, global buckling can be seen. In the middle picture, buckling of the cover layers can be seen, which leads to the detachment of large areas of the cover layers from the foam core. On the right, cover layer wrinkling has occurred. In this case, the test piece remains vertical and does not buckle. Small wrinkles form almost symmetrical to the sandwich center axis. In the area of the wrinkles, the cover layers become detached from the core. Local buckling behavior and wrinkling is the preferred failure type for energy absorption in sandwich elements stressed in the in-plane direction.

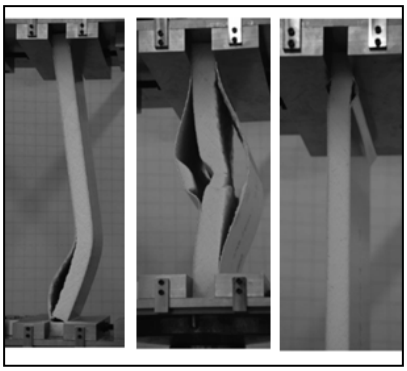

Fig. 7: Various types of failure in sandwich elements; left: global buckling of the test piece, center: cover layers detach and buckle, right: wrinkling and buckling behavior of the cover layers

In Fig. 8, a comparison is shown of various sandwich elements. The force level at the point of failure and the absorbed energy with respect to a defined distance are compared. All test pieces have a cover layer thickness of 0.3 mm. The foam density continued to be maintained. The core thickness was changed. It can be seen that all test pieces except for V1/19/03 are situated roughly on the same force and energy absorption level. The failure types of these test pieces were comparable to the global failure mechanisms shown in Fig. 7. However, test piece V1/19/03 fails on cover layer buckling behavior. This proves that cover layer wrinkling absorbs energy more effectively in comparison with the other failure options.

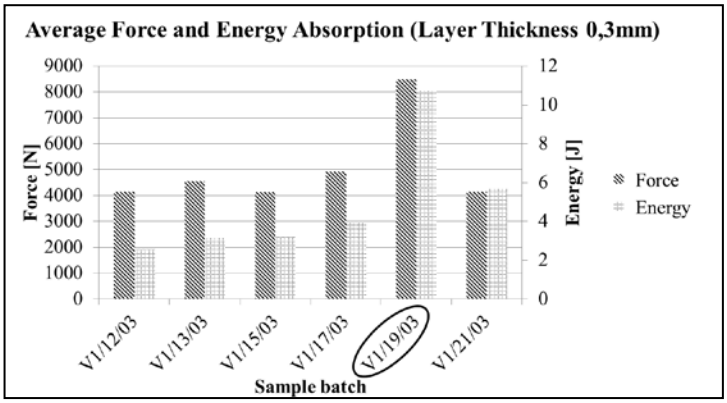

Fig. 8: Comparison of the failure forces and energies of various sandwich test pieces with a cover layer thickness of 0.3mm

Fig. 9 shows an example of a so-called failure mode map. Failure behavior can be predicted with the aid of a failure mode map. Failure is dependent on the core density (foam density) and the core thickness. In this simplified failure mode map, a distinction is made between global failure, shear failure and cover layer wrinkling. Detailed differentiation of the various global failure mechanisms is not necessary at this point, as the aim is cover layer wrinkling. The available failure mode maps are not applicable to the material combination being investigated here. Customized failure mode maps must therefore be drawn up. If the material behavior changes depending on the test speed, further differentiation is necessary.

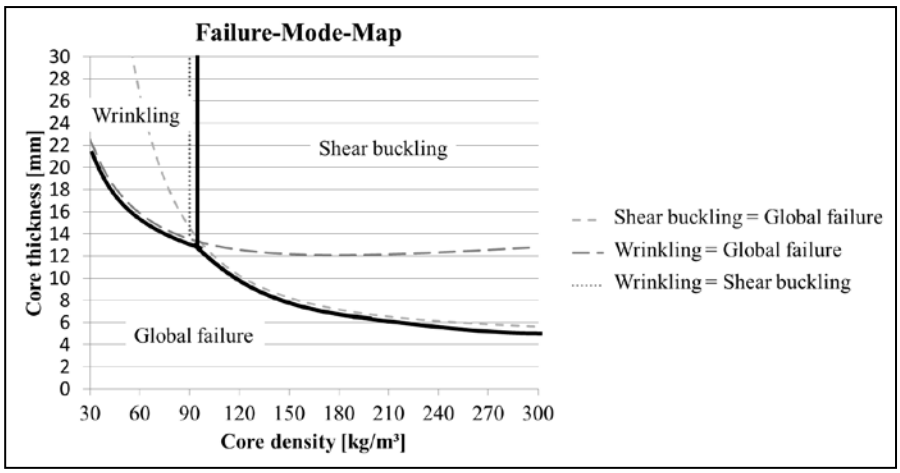

Fig. 9: Failure mode map, sample illustration, subdivided into global buckling, cover layer wrinkling and shear failure

Triggering mechanisms

In order to adjust the force level at the time of initial failure, so-called triggering mechanisms are employed. The reduction of peak force at the beginning of failure is important, for example, in keeping interior acceleration in a vehicle as low as possible. This results in lower deceleration, which acts on the occupants and means that the risk of injury can therefore be decreased. In metallic constructions, beading and nicking are used for triggering purposes. Beads are also conceivable in sandwich elements. In addition, the possibility exists of weakening sandwich components in a targeted manner by means of holes or slots (cf. Fig. 10).

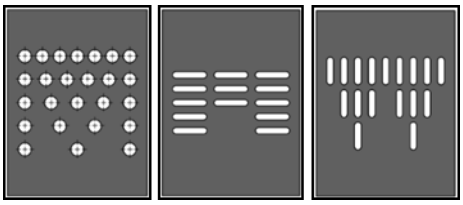

Fig. 10: Various types of triggering; left: hole pattern, center: horizontal slot, right: vertical slot

The use of external triggering mechanisms is also conceivable. These include, for example, wedge-shaped elements, which weaken the sandwich composite in the event of a desired failure at the frontmost edge and thus induce wrinkling of the cover layers. The effects of functioning triggering mechanisms are shown in Fig. 11. Pictured above is a two-row triggering mechanism with horizontal slots. Below left, a variant with holes and, below right, a design with vertical slots can be seen. In the case of the two-row triggering mechanism with horizontal slots, symmetrical wrinkles form. The apex of the wrinkles is in the top row of slots, the bottom end in the second row of slots. This

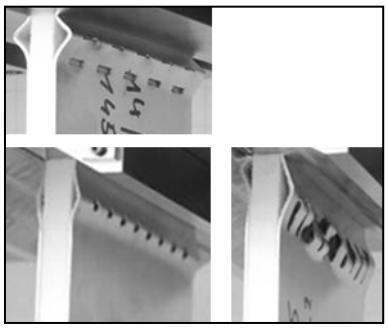

Fig. 11: Different triggering mechanisms; top: two-row slot triggering horizontally, below left: one-row hole triggering, below right: slot triggering vertically

can be accounted for by the weakening of the cover layers and easier buckling made possible as a result. The wrinkles in a test piece triggered with holes form completely symmetrically, both toward the sandwich center plane and toward the row of holes. In the case of a triggering mechanism with vertical slots, no symmetry toward the sandwich center plane is discernible. Moreover, the partitions between the slots do not buckle reproducibly. The triggering mechanism with vertical slots is nevertheless functional, as the test piece does not fail elsewhere.

Geometric influence on failure behavior

The findings from the preliminary observations were incorporated in component tests. Fig. 12 shows two different test pieces. Pictured on the left is a box with a square cross section which was triggered with a row of holes, as hole triggering mechanisms proved to be the most appropriate. Repeated wrinkling can be seen. As predicted, in the actual course of the test the triggering mechanism worked, i.e. the initial failure occurred on the triggering mechanism and spread out from there in the form of wrinkles in line with the progress of the deformation. Pictured on the right is a cruciform structure, which was tested untriggered. During the test, a rotary motion became apparent in the test piece, so that it became twisted. Nevertheless, wrinkles formed and no bending of the test piece was detected. The preliminary tests are being translated into the development of a complete vehicle body.

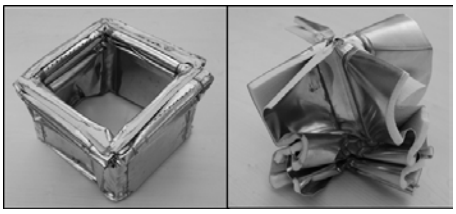

Fig. 12: Compression tests on test pieces with geometric variance; left: triggered box structure, right cruciform structure

New light weight and functional fillers

The first research contents in this article deal with polyurethane foam core materials. But on the other hand there are new materials which can be used in these applications. Aerogels are a new class of materials open new possibilities for core in sandwich materials. Aerogels are nanostructured open porous solids generally made via a sol-gel technology, meaning suitable liquids are mixing together such that sol formation starts and the colloidal particles aggregate to build a gel body which after suitable drying yields a nano-sponge, the aerogel [6].

They typically have densities in the range of 10 to 300 kg/m^3, strengths in the range of kPa to MPa, low thermal conductivity and a high capacity for sound absorption.

Fig. 13 shows an example of a polymeric aerogels in which silica aerogel particles are embedded yielding a light weight material with superisolating properties and good sound absorption.

If polymeric aerogels are used, made for instance from resorcinol resins, the density and their mechanical properties can be varied in a huge range. The densities prepared by us routinely lies between 60 and 200 kg/m^3 and their compression strengths are from 50 kPa to 300 kPa. If higher strengths are needed a few per mil by volume of cellulose microfibers can be embedded increasing the strength by a factor of 2-3. Such polymeric aerogels (RF-aerogels) can be used best as matrices for granulates or for felts or woven fabrics of all kinds and build a new class of composites. Introducing for instance silica aerogel granulates, which are commercially available [7] into the water-like polymeric matrix just before the transition form a sol to a gel, allows to incorporate 40 to 70 vol.% and vary thereby the density continuously between 100 kg/m^3 and 300 kg/m^3. An example of such a composite is shown in Fig. 13. The mechanical properties are then dependent not only on the matrix strength and the volume fraction of silica aerogel granulate, but also on the size of the granulate as shown in Fig. 14 and summarized in table 1.

Such type of aerogel composites were fabricated in arbitrary size and can easily be shaped mechanically or by direct casting in the sol-state to the shape needed. Compression test of these aerogels show a typical behavior of an open cell foam or a nano-sponge.

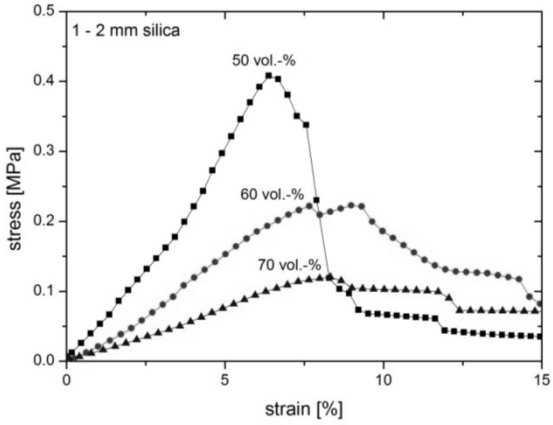

Fig. 14: Compression curves of RF-Aerogel-Silica Aerogel composites.

Table 1: Mechanical data of RF-Silica composites (see Fig.13)

Vol.% Silica granulate	Young's modulus [MPa]	Compression strength [kPa]
50	6.6	410
60	3.2	220
70	1.6	120

These type of aerogel-composites are currently tested in combination with metals as described above with respect to their combined mechanical behavior.

Metal-Aerogel porous structures

Another interesting approach for cores in sandwich structures opens on introducing heat resistant silica aerogel particles into an aluminum alloy melt thus producing a composite similar to a metallic foam, but being different since no foaming agent is needed and all pores are filled with a nanostructured open porous quartz-glass aerogel. We have produced such materials by various techniques. The most promising one is that of suction casting mimicking low-pressure die casting.

In suction casting we filled steel tubes of circular cross section with an inner diameter of 47 mm and a length of 500 mm with the aerogel granulates. The steel tube was placed above the top level of an AlSi11 melt, held at 700°C in a furnace that was covered like a chimney with heat resis

tant bricks as to heat up the tube to around 350 to 400°C. After 30 minutes of heating the tube was submerged into the melt bath. The melt was sucked in automatically and the steel tube could be withdrawn from the furnace after 30 seconds putting it then upside down for further cooling. Instead of a tube with a circular cross section we also used rectangular bars with a size of 30 x 20 mm with a wall thickness of 1.5 mm. The external steel tube could easily be removed and thus the Al-alloy-aerogel syntactic material be analyzed with respect to density, microstructure and mechanical properties. The Al-composite materials produced were examined with an x-ray tomography system.

Fig 15: Aerofims –Metal-Aerogel Composites made by suction casting.

Mechanical tests were performed with compression and three point bending test either using the naked Al-composite or within the steel tube and comparing it with hollow tubes or polymeric foam filled tubes.

Fig. 15 shows an example of samples after removal of the steel tube. One can clearly see that the matrix metal just fills interstices between the aerogel particles. The density of many samples was measured and typically lies between 0.94 – 1.03 g/cm^3. The porosities vary between 62 and 65 %. X-ray tomography, however, reveals that the filling by suction not always gave a complete filling.

Figure 16 shows two stress compression curves also depicting the variability, which we attribute to variations in the production process and therefrom the materials microstructure.

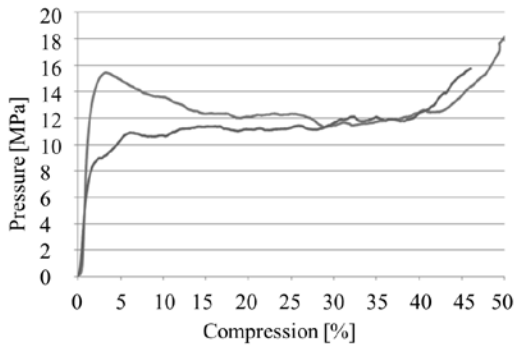

Figure 16: stress compression curves of two AlSi11-Aerogel composites

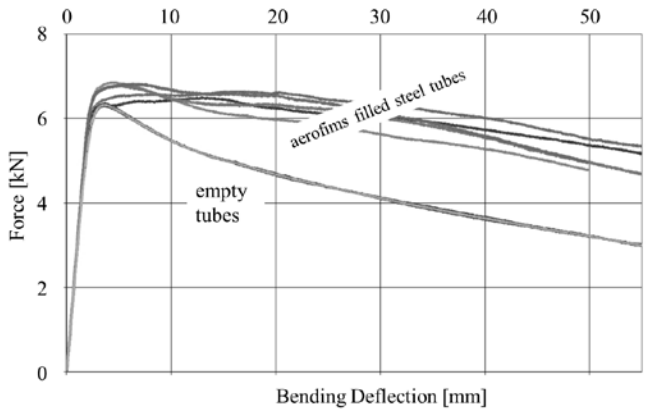

Figure 17: Bending test on rectangular steel bars filled with aerogel syntactic foams.

The yield strength varies between 6.9 and 11.5 MPa. After yielding the typical plateau stress regime is observed having an extent from 5 and 40 % plastic deformation, as to be expected from porous solids and as attributed typically to the collapse of the metallic lamellae separating the pores, which

are in this case the aerogel particles. The energy absorption up to 40% plastic deformation turns out to vary between 4.5 and 5.1 kJ/kg.

With the series of test with rectangular steel tubes we tested the three point bending behavior. Figure 17 shows the load deformation curves for the series with an aerogel-metal core compared to empty steel tubes.

The curves of the empty tubes behave as expected. There first is a linear increase in force needed to bend the bars elastically, followed by a short yielding and then the maximum in force is reached once buckling starts, which then is followed by a decrease in force needed to further bend the bar. The metal-aerogel-core inside, however, introduces a long period of deformation before the force decreases.

Calculating from these curves the energy taken up by the bars as a function of deflection and comparing the energy-deflection of the empty bar and those of the two aerogel-metal composites with different aerogel particle size, shows that the composite with the smaller aerogel particles yield a better energy uptake (at the same volume content). Compared to the empty tubes, the aerogel core increases the energy absorption by about 60%. We attribute this to two effects: first of course the energy uptake during deformation of the core, but second also due to a modified deformation of the steel tube, which does not buckle compared to the empty one, but deforms further until cracks develop.

Vehicle concept in sandwich design

The Institute of Vehicle Concepts is developing a new kind of vehicle concept using sandwich construction. The virtual vehicle structure is shown in Fig. 18. The front end and rear structures of the vehicle are constructed from sandwich panels and are comparable to the test pieces shown in Fig. 12. Triggering mechanisms in the form of hole patterns are also used. The vehicle is designed to be driven by a battery fuel cell system. The aim is a very light and secure vehicle structure. First structural components were tested on the facilities of the institute. Fig. 19 shows the front structure of the LUV (Light Urban Vehicle) before and after crash test. The deformed structure shows the wrinkling of the aluminum layers. The crash speed was 9.5 m/s and 38 kJ of energy were absorbed bei deformation. The displacement lenght is 350 mm.

Fig. 19: Front structure of the LUV before and after crash test

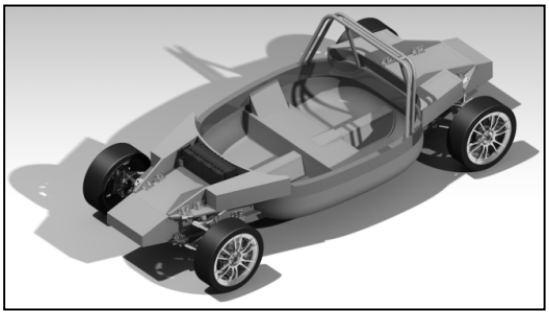

Fig. 18: Vehicle concept in a new kind of sandwich construction

Summary and outlook

Beginning with generic tests on foam and sandwich elements, via the investigation of triggering mechanisms for the targeted weakening of sandwich components and the application of the findings to box and cruciform structures, through to the conception of a complete vehicle using sandwich construction, it could be shown that sandwich materials and an appropriate construction have the potential to be used in automobile manufacture.

The performance of the sandwich materials and of the construction must be validated in ongoing actual tests. More tests on foam materials, sandwich elements and sandwich components are necessary. Also the simulation process and the used parameters in it have to be validated. A matching joining technology has to be detected to guarantee the performance of the sandwich structures and to achieve the objective of an overall body in white structure in sandwich design.

References

[1] Wiedemann, J.: Motor Vehicles I, Lecture notes, University of Stuttgart

[2] Zenkert, D.: An Introduction to Sandwich Construction. 1st edition. EMAS, London,1997.

[3] Starlinger, A.: Development of Efficient Finite Shell Elements for Analysis of Sandwich

Structures under Large Instabilities. VDI-Verlag GmbH, Düsseldorf, 1991.

[4] DIN EN ISO 844: Harte Schaumstoffe – Bestimmung der Druckeigenschaften; Rigid cellular plastics – determination of compression properties; October 2009

[5] DIN 53292: Zugversuch senkrecht zur Deckschichtebene; Testing of sandwiches; tension test in flatwise plane; February 1982

[6] M.Aegerter (Ed.), Handbook Aerogels, Springer, New York 2012

[7] Cabot Aerogels, see http://www.cabot-corp.com/aerogel